

Sensitivity to the KARMEN timing anomaly at MiniBooNE

S. Case

Columbia University, New York, New York 10027

S. Koutsoliotas and M. L. Novak

Bucknell University, Lewisburg, Pennsylvania 17837

(Received 2 August 2001; published 28 February 2002)

We present sensitivities for the MiniBooNE experiment to a rare exotic pion decay producing a massive particle Q^0 . This type of decay represents one possible explanation for the timing anomaly reported by the KARMEN Collaboration. MiniBooNE will be able to explore a region of the KARMEN signal that has not yet been investigated.

DOI: 10.1103/PhysRevD.65.077701

PACS number(s): 14.80.-j, 12.60.-i, 13.20.Cz, 13.35.Hb

I. THE KARMEN TIMING ANOMALY

The KARMEN Collaboration at the ISIS spallation neutron facility at the Rutherford Appleton Laboratory uses a pulsed neutrino beam from stopped pion and muon decays to study neutrino-nucleon interactions. They have reported an anomaly in the timing distribution of neutrino interactions from stopped muon decays [1]. One possible explanation for the anomaly is an exotic pion decay where a neutral and weakly interacting or sterile particle (Q^0) with a velocity of $4.9 \text{ m}/\mu\text{s}$ is produced. This particle, with a mass of $33.9 \text{ MeV}/c^2$ measured from the time of flight, then decays in the KARMEN detector to $e^+e^-\nu$ or $\gamma\nu$. The decay to $e^+e^-\nu$ is strongly favored by recent data [2].

The KARMEN experiment reports a signal curve for pion branching ratio $B(\pi \rightarrow \mu Q^0) \times B(Q^0 \rightarrow \text{visible})$ versus lifetime. A minimum branching ratio of 10^{-16} exists for a lifetime of $3.6 \mu\text{s}$. Two solutions exist above this minimum: one at large lifetime and one at small lifetimes. Experiments at the Paul Scherrer Institute (PSI) have excluded any exotic pion decays to muons with branching ratios above 6.0×10^{-10} at 90% C.L., and to electrons with branching ratios above 9.0×10^{-7} at 90% C.L. [3–5]. Also, the NuTeV experiment (E815) at Fermi National Accelerator Laboratory (Fermilab) has excluded the short lifetime solution with branching ratios above 5×10^{-12} at 90% C.L. [6]. Still, segments of the KARMEN signal region remain to be addressed.

Although recent data from KARMEN2 do not show a statistically significant signal for the Q^0 particle, a substantial effect persists in the combined data sets from KARMEN1 and KARMEN2 [7].

II. THE MiniBooNE EXPERIMENT

The MiniBooNE experiment (E898), currently under construction at Fermilab, will begin collecting data in 2002. The Fermilab Booster ring will provide 8 GeV protons, which will strike a beryllium target. This interaction will produce primarily pions, which will decay in flight in a 50-m decay pipe. Muons from the pion decays will be stopped in a steel beam dump and about 489 m of earth between the decay pipe and the center of the MiniBooNE detector. The MiniBooNE

detector is a spherical tank, 6.1 m in radius, and filled with 807 tons of mineral oil. An inner tank structure at 5.75 m radius supports 1280 8-inch photomultiplier tubes facing into the tank. An additional 330 8-inch photomultiplier tubes in the optically isolated outer region of the tank will serve as a veto shield. The MiniBooNE experiment will receive approximately 5×10^{20} protons on target each year.

A GEANT-based [8] Monte Carlo program was used to simulate the production and decay of the Q^0 particles from pion decay using the decay mode $Q^0 \rightarrow e^+e^-\nu$. Figure 1 shows the energy spectrum of all pions produced in our model. “Parent pions” which produce Q^0 s within the detector acceptance, and the Q^0 particles that reach our detector are also shown. The number of Q^0 s decaying in the MiniBooNE detector in a year of running was then calculated for a variety of lifetimes and branching ratios within the KARMEN signal band. The electron and the positron will repre-

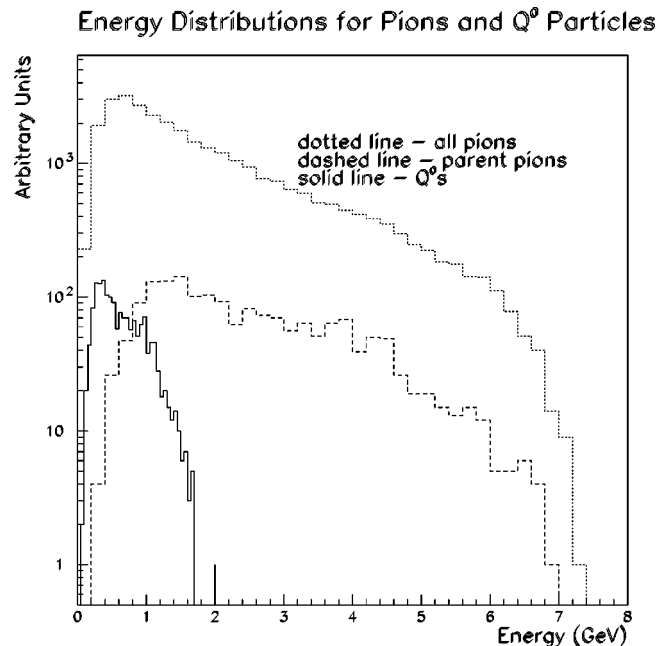


FIG. 1. Energy distributions for particles in the Monte Carlo model. The distribution for all pions produced, the pions which decay to Q^0 s within the detector acceptance, and the Q^0 energy spectrum are shown.

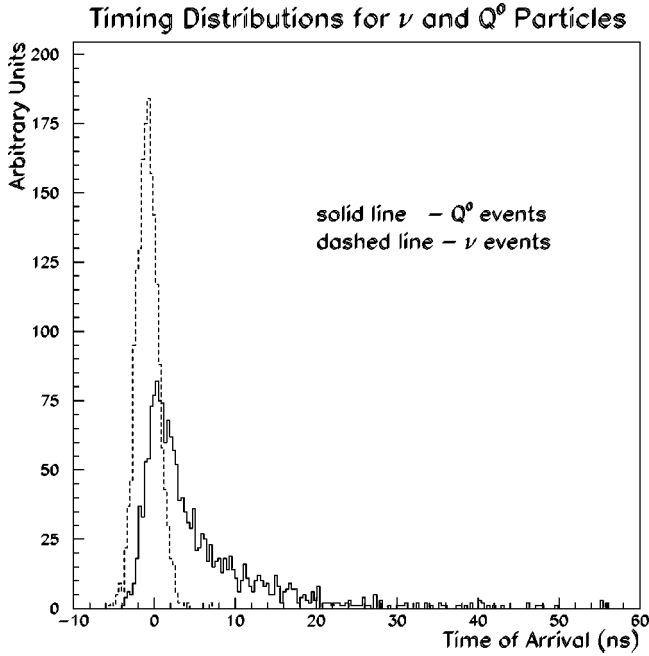


FIG. 2. Timing distribution for events at the MiniBooNE detector. The solid line represents the Q^0 particles, and the dashed line shows the distribution of neutrinos from the beam.

sent the signal signature and will be reconstructed from their Cerenkov rings in the detector. In most cases, the opening angle between the electron and the positron appears to be too small to resolve into two separate Cerenkov rings. Consequently, the major background to the Q^0 signal will be ν_e quasielastic scattering. In the cases where the two rings are separately resolvable, neutral current π^0 production will be the dominant background contribution.

III. THE BOOSTER TIMING STRUCTURE

The timing structure of the proton pulses from the Booster allows us to discriminate between neutrino and Q^0 events. Micropulses within the Booster pulses can be approximated by Gaussian-shaped pulses with widths of 1.5 ns, separated by 18.94 ns. Given that the Q^0 mass is very close to the kinematic limit for the decay $\pi \rightarrow \mu Q^0$, the Q^0 particles will be traveling at speeds similar to the parent pions, and considerably slower than the neutrinos. Most of the neutrinos will arrive at the detector within a tight timing bunch, while many of the Q^0 s will reach the detector at times between the neutrino bunches. Figure 2 shows the timing distributions for a neutrino bunch and for the corresponding Q^0 particles, and Fig. 3 shows the arrival time of the Q^0 particle as a function of the energy of the parent particle. The timing structure makes it possible to impose a cut on the time of arrival which is very effective in isolating the Q^0 signal. By varying the value of the timing cut, the Q^0 detection efficiency was examined. Figure 4 shows the efficiency of detecting a Q^0 particle as a function of neutrino rejection. We have assumed MiniBooNE's timing resolution for neutrino events to be 1.2 ns and independent of neutrino energy.

This paper presents sensitivities of the MiniBooNE ex-

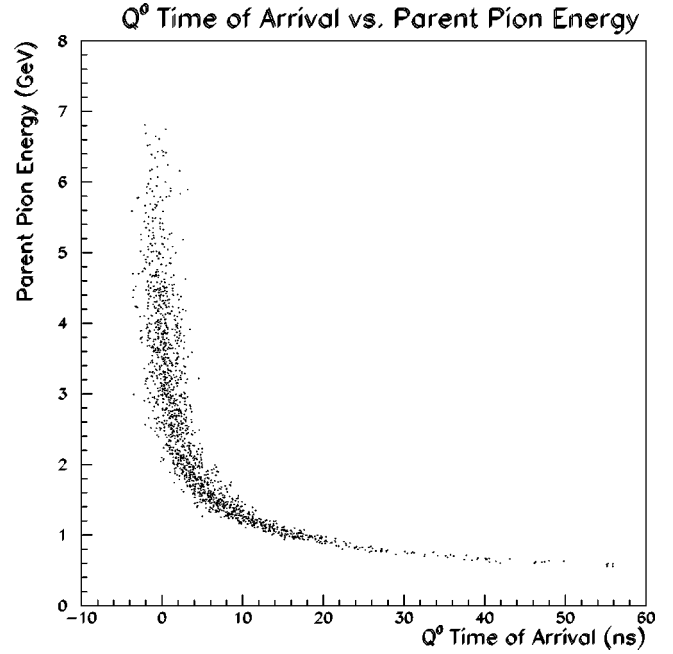


FIG. 3. The Q^0 time of arrival at the MiniBooNE detector as a function of the energy of the parent pion.

periment to the KARMEN timing anomaly based on Q^0 efficiencies of 10% and 100%. It is anticipated that the final MiniBooNE sensitivity will lie between these limits. For this analysis we also assume no backgrounds to the Q^0 signal.

IV. MiniBooNE SENSITIVITY TO THE KARMEN TIMING ANOMALY

MiniBooNE will be able to explore the short-lifetime region of the KARMEN signal at 90% C.L. down to branching

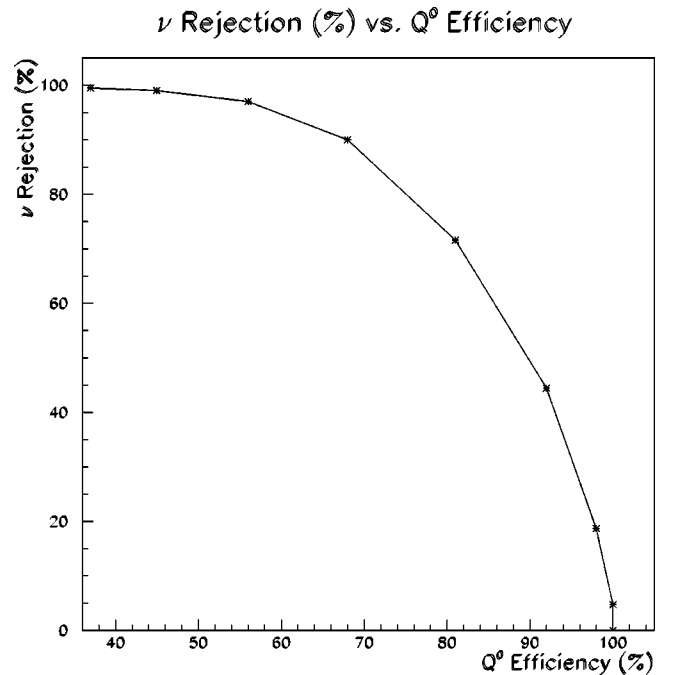


FIG. 4. The ν rejection (%) vs Q^0 efficiency for different timing cut values.

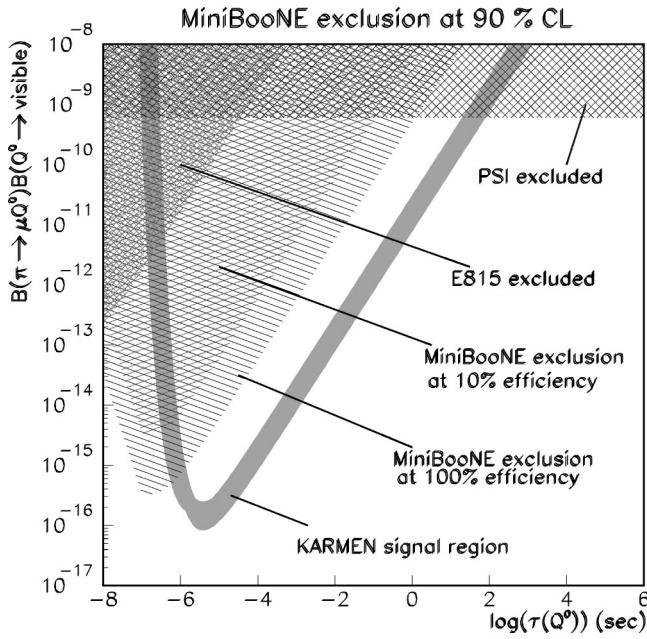


FIG. 5. MiniBooNE's exclusion reach at 90% C.L. based on one year of running and assuming no background.

ratios of approximately 5×10^{-15} at 10% detection efficiency. Figure 5 shows MiniBooNE's exclusion region from one year of running and assuming no background. MiniBooNE's maximum reach in the short-lifetime solution may be extended to a branching ratio of 5×10^{-16} if 100% detection efficiency is assumed. These limits are based on a preliminary version of the reconstruction algorithm. Improvements to the sensitivity are anticipated with further development of the reconstruction algorithm.

Our single event sensitivity in the short-lifetime solution will reach branching ratios of approximately 2×10^{-15} at 10% detection efficiency in one year of running, with no background. The maximum single-event sensitivity (based on 100% detection efficiency) will reach branching ratios of

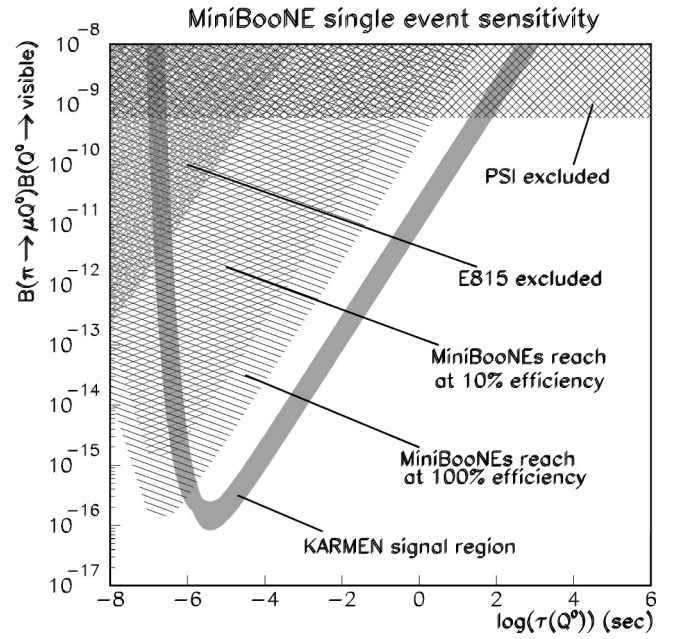


FIG. 6. MiniBooNE's single-event sensitivity in one year of running, assuming no background.

approximately 2×10^{-16} in one year of running with no background (Fig. 6).

In conclusion, the timing anomaly observed by the KARMEN1 experiment has yet to be explained. The MiniBooNE experiment will be capable of probing previously unexplored regions of the KARMEN signal.

ACKNOWLEDGMENTS

The authors thank the E898 (MiniBooNE) Collaboration, with special thanks to J. M. Conrad, J. A. Formaggio, M. H. Shaevitz, and E. D. Zimmerman of Columbia University. We also thank the National Science Foundation for their support.

- [1] B. Armbruster *et al.*, Phys. Lett. B **348**, 19 (1995).
- [2] C. Oehler, Nucl. Phys. B (Proc. Suppl.) **85**, 101 (2000).
- [3] M. Daum *et al.*, Phys. Lett. B **361**, 179 (1995).
- [4] N. De Leener-Rosier *et al.*, Phys. Rev. D **43**, 3611 (1991).
- [5] M. Daum *et al.*, Phys. Rev. Lett. **85**, 1815 (2000).
- [6] J.A. Formaggio *et al.*, Phys. Rev. Lett. **84**, 4043 (2000).

- [7] K. Eitel *et al.*, Nucl. Phys. B (Proc. Suppl.) **91**, 191 (2001); K. Eitel (private communication); R. Schrock (private communication).
- [8] Applications and Software Group, CERN, "GEANT: Detector Description and Simulation Tool," CERN Program Library Report Q123.